Radiocarbon in the Northern Indian Ocean two decades after GEOSECS

Koushik Dutta[1,2] and Ravi Bhushan[1]

Received 23 December 2010; revised 16 September 2011; accepted 19 March 2012; published 18 May 2012.

[1] The ^{14}C measurements in the Arabian Sea and the Bay of Bengal during the late 1990s offer a way to assess the temporal changes in the inventories of bomb-^{14}C and its penetration into the ocean, in two decades since GEOSECS expeditions (1977–1978). The mean penetration depth of bomb radiocarbon during GEOSECS (1977–1978) was 270 m, which increased by ~40% to 381 m in 1994–1998. The small changes in bomb-^{14}C inventories, significant increase in the mean penetration depths and lowering of the surface $\Delta^{14}C$ values in the northern Indian Ocean indicate the temporal variation of bomb-^{14}C in two decades is mainly through downward transfer through mixing with deeper waters. The observed bomb-^{14}C inventory in the northern Indian Ocean agrees with numerical model simulated values, except at the equatorial Indian Ocean. The high bomb-^{14}C inventory at the equator can be attributed to lateral advection of ^{14}C-enriched waters from the Pacific Ocean through the Indonesian archipelago. The air-sea CO_2 exchange rates in the northern Indian Ocean calculated from the bomb-^{14}C inventories range from ~7 mol m^{-2} yr^{-1} (in the northern Bay of Bengal) to 20 mol m^{-2} yr^{-1} (in the equatorial Indian Ocean). Net sea-air flux of CO_2 estimated for the northern Indian Ocean between 0° and 25°N is ~104 ± 30 TgC yr^{-1}. The Bay of Bengal is a net sink of atmospheric CO_2 (~−1 ± 0.4 TgC yr^{-1}), while the Arabian Sea is a source of CO_2 (~69 ± 21 TgC yr^{-1}).

Citation: Dutta, K., and R. Bhushan (2012), Radiocarbon in the Northern Indian Ocean two decades after GEOSECS, *Global Biogeochem. Cycles*, *26*, GB2018, doi:10.1029/2010GB004027.

1. Introduction

[2] The naturally occurring radioactive isotope of carbon ^{14}C, commonly known as radiocarbon, can be used as a tracer to study the pathways of carbon across various exchangeable carbon reservoirs (e.g., oceans, biosphere, soil organic matter), which interact with atmospheric CO_2 reservoir on time scale of decades to centuries [*Stuiver et al.*, 2000]. The inadvertent addition of bomb-^{14}C in the environment between early 1950s and 1960s from above ground nuclear detonations can be used to address a host of problems pertaining to the global carbon cycle and ocean circulation. Since late 1950s global surface oceans showed a measurable increase in ^{14}C concentration due to transfer of bomb-^{14}C from the atmosphere to the oceans [*Rafter and Ferguson*, 1957]. ^{14}C in oceans has long been employed as a useful tracer to study the processes of air-sea CO_2 exchange and circulation at different time scales. Both natural (cosmogenic) and bomb produced (anthropogenic) ^{14}C are suitable for these studies.

[3] The increase in oceanic inventory of bomb-^{14}C depends on the local air-sea CO_2 exchange rate, diffusivity, vertical and lateral movement of seawaters. Since the bomb-^{14}C concentration in the upper layers of the ocean changes on time scale of decades, it is an ideal tracer to study air-sea CO_2 exchange processes and to trace decadal mixing processes in the thermocline [*Quay and Stuiver*, 1980; *Broecker et al.*, 1985, 1995; *Druffel*, 1989]. Measurement of ^{14}C in oceans is also important for validating ocean general circulation models that are primarily used for predicting oceanic CO_2 uptake rates and used to simulate the oceanic ^{14}C distribution [*Toggweiler et al.*, 1989; *Jain et al.*, 1995; *Guilderson et al.*, 2000; *Sweeney et al.*, 2007].

[4] The Arabian Sea and the Bay of Bengal in the northern Indian Ocean are characterized by contrasting oceanographic features, which result in distinct differences in their circulation pattern in the thermocline region and also in the magnitude and direction of the sea-air CO_2 fluxes. The Bay of Bengal receives large amount of fresh water throughout the year from seven major rivers, with peak input during the southwest monsoon season (June to September). Large inputs of fresh water causes formation of a low salinity and low-density layer at the surface Bay of Bengal, thereby creating a steep gradient of the isopycnal surfaces and reducing the vertical mixing. This, coupled with high biological

[1]Geosciences Division, Physical Research Laboratory, Ahmedabad, India.
[2]Now at Large Lakes Observatory, University of Minnesota, Duluth, Duluth, Minnesota, USA.

Corresponding author: R. Bhushan, Geosciences Division, Physical Research Laboratory, Navrangpura, Ahmedabad 380 009, India. (bhushan@prl.res.in)

0886-6236/12/2010GB004027

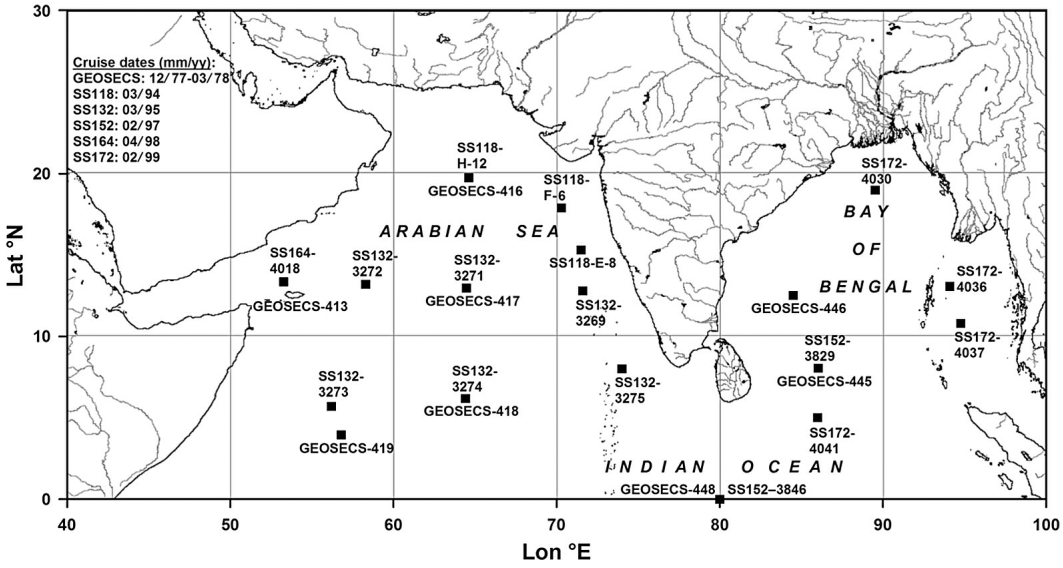

Figure 1. Sampling locations of FORV *Sagar Sampada* cruises in the northern Indian Ocean between 1994 and 1999, showing the GEOSECS reoccupation stations.

productivity keeps the surface seawater pCO_2 in this oceanic region lower than that in the atmosphere, making it a sink of atmospheric CO_2 [*Kumar et al.*, 1996]. Whereas in the Arabian Sea the pCO_2 of the surface waters is greater than that in the atmosphere due to strong wind induced upwelling of CO_2 rich deep waters, thus making it a net source of CO_2 to the atmosphere [*Kumar et al.*, 1992; *Sarma et al.*, 1998, 2000; *Takahashi et al.*, 2009]. These contrasting physical oceanographic settings and the wind speed regimes of the two basins influence the regional ocean-atmosphere fluxes of CO_2. In addition, these also influence the isotopic composition of carbon in the concerned reservoirs, i.e., both in the oceanic dissolved inorganic carbon (DIC) as well as in the atmospheric CO_2 overlying this ocean. Complex and contrasting ocean circulation patterns in the Arabian Sea and the Bay of Bengal complicate the modeling of the distribution of tracers in this region. The first measurements of ^{14}C in the water column of the Arabian Sea and the Bay of Bengal were done during 1977 and 1978, as a part of the international GEOSECS program [*Stuiver and Östlund*, 1983]. Based on reoccupation of three Arabian Sea GEOSECS stations, *Bhushan et al.* [2000] described temporal changes in radiocarbon distribution about two decades after GEOSECS.

[5] To study the temporal changes in the distribution of radiocarbon in the Arabian Sea and the Bay of Bengal, three expeditions were made between 1997 and 1999 onboard FORV *Sagar Sampada* (Figure 1). During 1997 (cruise SS-152), three GEOSECS stations were reoccupied—one in the equatorial Indian Ocean and the other two in the central Bay of Bengal. In 1998 (cruise SS-164), GEOSECS stations in the Arabian Sea were reoccupied including one station in the Gulf of Aden near the Red Sea mouth. During 1999 (SS-172) stations in the northern and the southern Bay of Bengal and the Andaman Sea were occupied. Samples of seawater were collected in vertical profiles for measurements of ^{14}C in DIC. CO_2 were also collected from the maritime air during these cruises for $^{14}CO_2$ measurements. Here we report the observed changes of ^{14}C in DIC of the northern Indian Ocean in two decades since the GEOSECS expedition. From the distributions of bomb-^{14}C in the upper ocean, we have estimated net sea-air flux of CO_2 for the northern Indian Ocean.

2. Material and Methods

2.1. Sampling of Seawater

[6] Seawater samples were collected using 30 lit PVC *Go-Flo* bottles (*General Oceanics*, Miami, Florida, USA) attached with a 12-position rosette fitted with eight bottles. Continuous profiles of temperature, salinity and dissolved oxygen were obtained using a CTD (conductivity-temperature-depth) profiler. From the raw CTD data, potential temperature (θ) and potential density (σ_θ) were derived using the software package SEASOFT (v. 4.232). The CTD temperature and salinity values are expressed following the conventions of ITS-90 (degree Celsius) and PSS-78 (Practical Salinity Scale), respectively. The dissolved oxygen and salinity values from CTD were calibrated by comparing the onboard measurements of O_2 by Winkler's titration and salinity by *Autosal* salinometer in collected seawater samples. Water samples were collected from selected depths, from the surface ($\sim$5 m) to a few hundred meters above the seafloor guided by the CTD profiles. Usually two samples were collected from each cast by tripping four 30 lit bottles at the desired depth, thus collecting about 120 lit of seawater for each depth. Aliquots of this sample were used for measurements of various parameters.

2.2. Analyses of Nutrients (Silicate, Total Nitrate and Phosphate)

[7] About 500 ml of seawater was used for the analysis of dissolved silicate, total nitrate (nitrate + nitrite) and phosphate [*Strickland and Parsons*, 1972]. The samples were kept refrigerated prior to analysis. Silicate and nitrate were measured onboard using a *Technicon* auto-analyzer. Phosphate was measured by spectrophotometry using a *Beckman*

model 26 spectrophotometer. Based on repeat measurements of seawater samples, the precisions ($\pm 1\sigma$) of silicate, total nitrate and phosphate measurements were 1.34%, 1.36% and 1.63%, respectively of the measured values. Accuracies of silicate and nitrate measurements were about ±5%, as checked by analyzing *CSK* standard solutions (Wako Chemical Industries Ltd., Japan).

2.3. Analysis of Total Dissolved Inorganic Carbon (ΣCO_2)

[8] An aliquot of seawater sampled from each depth in the PVC *Go-Flo* bottles were collected in 125 ml *Borosilicate* glass bottles. Immediately after collection the samples were poisoned with 25 μl of saturated mercuric chloride solution to halt biological production. The bottles were sealed with ground glass stoppers (greased with *Apeizon-N* grease) and kept refrigerated at ~2°C until analysis. ΣCO_2 was measured in the samples using a *UIC model 5012* CO_2 coulometer (UIC Inc., Joliet, Illinois, USA) [*Körtzinger et al.*, 1999]. Based on repeat analyses of seawater samples, typical precision of ΣCO_2 measurements was ±3 μmol kg^{-1} (1σ). The accuracy of ΣCO_2 measurements was checked from analyses of certified reference seawater (Batch#42, December, 1997, supplied by Prof. Andrew G. Dickson of Scripps Institute of Oceanography, USA). The mean ΣCO_2 measured during this study for this standard seawater is 1983.2 ± 2.3 μmol kg^{-1} (1σ, n = 20), in good agreement with its certified value of 1985.1 ± 0.8 μmol kg^{-1}.

2.4. Radiocarbon Analysis

[9] ^{14}C in the seawater DIC samples were measured using conventional liquid scintillation counting (LSC) technique. Details of the method are discussed in *Dutta* [2001]. About 100 lit of seawater sample were taken for each ^{14}C analysis. DIC was extracted onboard from the seawater soon after sample collection using a closed circulation system to minimize exchange and contamination with atmospheric CO_2. In the laboratory the extracted DIC were converted to benzene for ^{14}C assay, following the procedures outlined in *Noakes et al.* [1965] and *Gupta and Polach* [1985]. Details of the LSC methods were described by *Bhushan et al.* [1994]. The ^{14}C results are expressed as $\Delta^{14}C$ permil (‰) as per the conventions outlined by *Stuiver and Polach* [1977]. The internal precision (1σ) of the $\Delta^{14}C$ measurements based on modern samples (using 3 ml of benzene) was ±5‰.

3. Depth Profiles of ^{14}C in DIC of the Northern Indian Ocean

[10] The depths sampled for ^{14}C analysis are indicated in the θ-S plots of Figure 2, which show the water masses sampled. The measured $\Delta^{14}C$ profiles (filled circles with $\pm 1\sigma$ errors) are shown in Figure 3. The reconstructed prenuclear $\Delta^{14}C$ profiles for these stations are given as dashed lines (method described in Appendix A). Significant decrease in the $\Delta^{14}C$ values were observed in the surface Bay of Bengal in two decades after the GEOSECS expedition of 1977–1978 (Figure 4). During 1997 and 1999, the $\Delta^{14}C$ values of the surface waters (at ~5 m) ranged from 57‰ in the southern Bay of Bengal (SS172–4041) to a minimum of 18‰ in the northern Bay of Bengal (SS172–4030). The mean surface $\Delta^{14}C$ values for the Bay of Bengal stations between 9°N to 20°N were about 40‰; while $\Delta^{14}C$ in the surface equatorial Indian Ocean (SS152–3846) was 55‰. These are lower by ~60‰ to 80‰ than those measured during 1978, comparing the values at GEOSECS stations 445 and 448 (Table 1). The $\Delta^{14}C$ decrease observed in the surface Arabian Sea was ~30‰. During the GEOSECS expedition significant contrast was seen between the surface $\Delta^{14}C$ values of the Arabian Sea (59 to 95‰) and the Bay of Bengal (107 to 117‰). This difference became insignificant after two decades, when the surface Arabian Sea recorded $\Delta^{14}C$ values of 40 to 58‰ during 1994 and 1995, compared to 40 to 57‰ in the Andaman Sea and the southern Bay of Bengal during 1997 and 1999 (Figure 5) [*Bhushan et al.*, 2000; *Dutta et al.*, 2007]. The reduction in the surface $\Delta^{14}C$ values can be partly attributed to the lowering of the atmospheric $\Delta^{14}C$ from ~300‰ during 1978 [*Nydal and Lövseth*, 1996; *Chakraborty et al.*, 2008] to ~90‰ in late 1990s [*Bhushan et al.*, 1997; *Dutta et al.*, 2006], and transfer of ^{14}C-enriched waters from the surface to the deeper layers through vertical mixing. The later process appears to play a major role in the northern Indian Ocean as evidenced from the changes in the mean penetration depths of bomb-^{14}C.

[11] Lowest surface $\Delta^{14}C$ in the Bay of Bengal measured at the station SS172–4030. This station is located closest to the Ganges-Brahmaputra delta, which receives large fresh water inputs both through river discharge as well as submarine groundwater discharge. The low $\Delta^{14}C$ values measured at this station are most likely due to mixing with large amount of submarine groundwater discharge with old ^{14}C-age. *Ravi Prasad et al.* [2008] had reported ^{14}C-ages ranging from 3040 BP to 9025 BP for groundwater samples collected from Orissa state, not far from the northeastern Bay of Bengal. In absence of detailed $\Delta^{14}C$ measurements in the Ganges-Brahmaputra river system, it is difficult to assess the riverine contribution to depleted $\Delta^{14}C$ values in the northern Bay of Bengal.

[12] In all stations of the Bay of Bengal a distinct maxima of $\Delta^{14}C$ was seen at depths of 70~100 m, with $\Delta^{14}C$ values of ~60 to 70‰. The subsurface maxima was developed due to gradual downward transfer of the surface bomb-^{14}C transient to deeper levels, and subsequent equilibration of the surface water with atmospheric CO_2 with progressively lower $\Delta^{14}C$ values. This feature was not seen in the northern Bay of Bengal (SS172–4030) probably due to rapid replenishment of the surface waters resulting from voluminous fresh water discharge. Such subsurface maxima could not be resolved in the Arabian Sea $\Delta^{14}C$ profiles obtained during 1994–1995 due to coarser sampling resolution. However, it is unlikely that such feature could develop in the Arabian Sea. The isopycnal gradient of the surface waters is much less in the Arabian Sea than in the Bay of Bengal, aiding vertical mixing of waters and hence more rapid transfer of ^{14}C-enriched waters from the surface to deeper levels, thus preventing formation of any distinct subsurface $\Delta^{14}C$ maxima in the Arabian Sea.

[13] From the GEOSECS measurements, no significant changes in the deep-water $\Delta^{14}C$ values of the northern Indian Ocean stations are seen from the present study, except for the station SS164–4018 (reoccupation of GEOSECS 413), near the Gulf of Aden. The intermediate water between

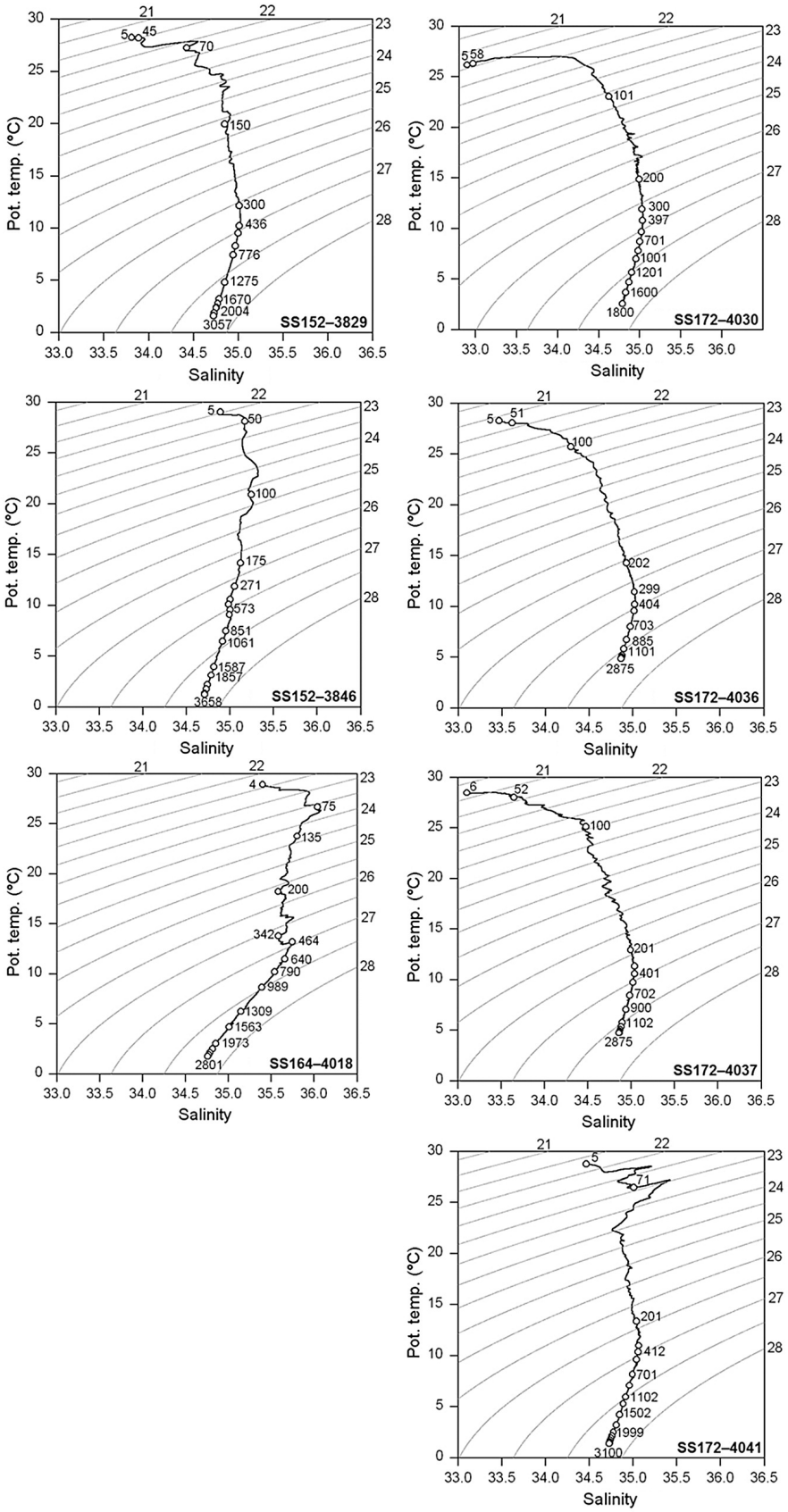

Figure 2. Potential temperature-salinity ($\theta-$S) plots of the stations in the northern Indian Ocean. The circles indicate the depths sampled for ^{14}C measurements. The contours indicate potential density (σ-θ, top and left axes).

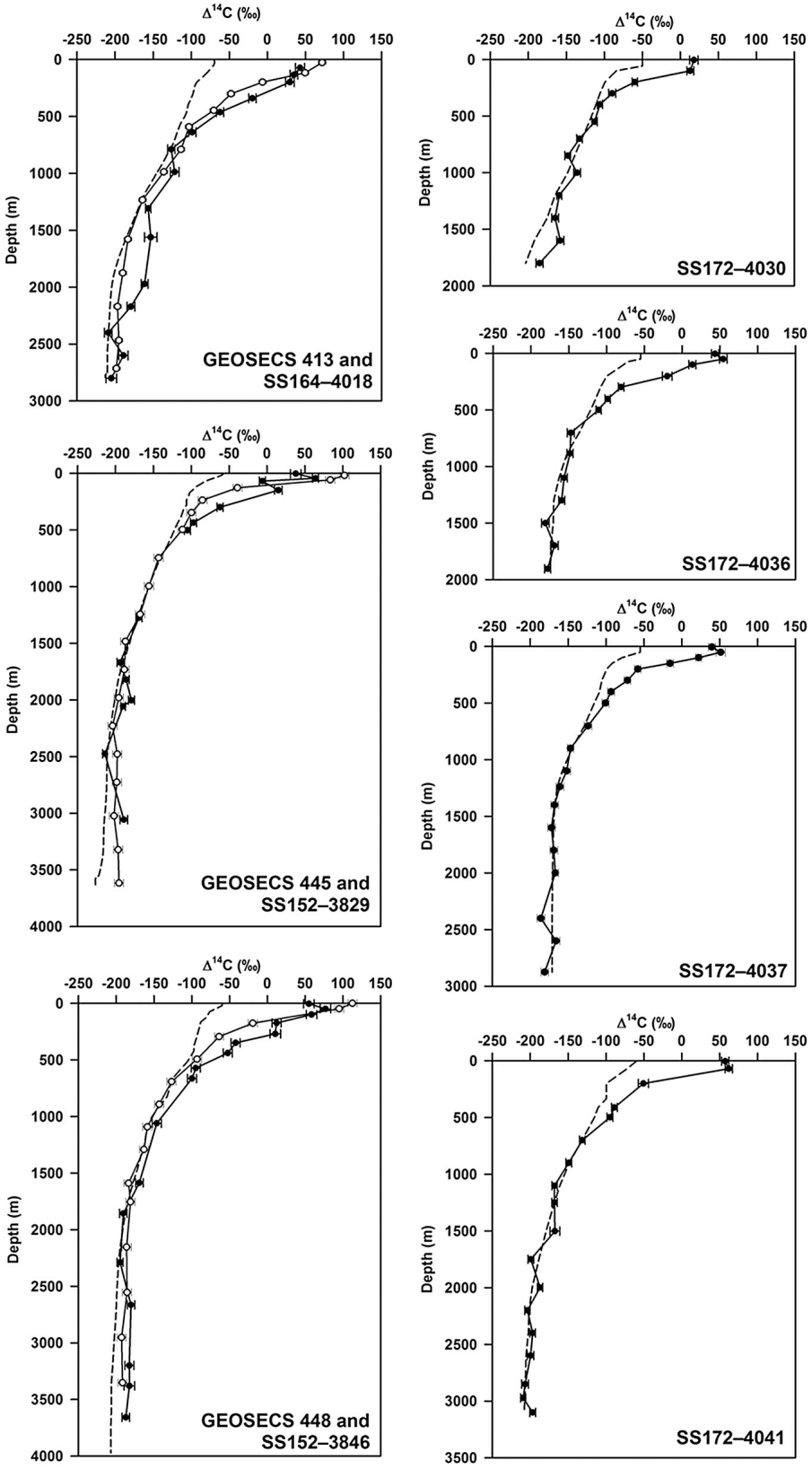

Figure 3. Depth profiles of $\Delta^{14}C$ in DIC at the northern Indian Ocean stations. Filled circles are the results obtained for this study. Open circles are data obtained during the GEOSECS expeditions [*Stuiver and Östlund*, 1983]. The dashed lines are pre-bomb $\Delta^{14}C$ reconstructed from silicate data.

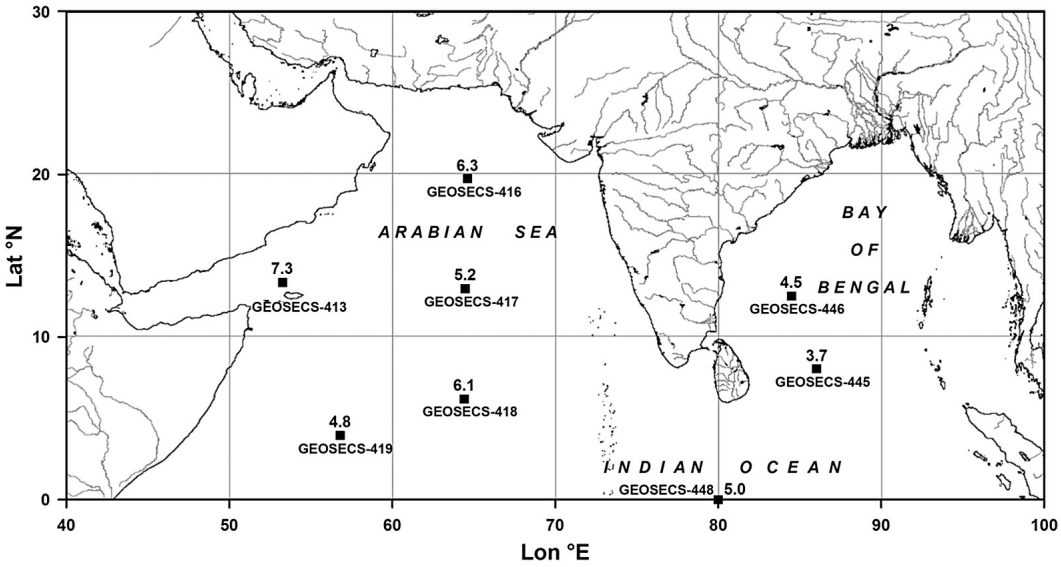

Figure 4. Bomb-^{14}C inventories ($\times 10^9$ atoms cm^{-2}) in the northern Indian Ocean as calculated in this study for the GEOSECS stations occupied in 1977–1978.

1200 to 2200 m depths in this station has shown an increase of Δ^{14}C by ~40‰ from the values measured during 1977 [*Bhushan et al.*, 2003]. This increase is most likely due to gradual sinking of more saline and dense Red Sea surface water (RSW), with higher Δ^{14}C to deeper depths. The mixing proportion of RSW between 1200 and 2200m depths near the location of SS164–4018 is 5 to 20%, as seen from multi parametric water mass analyses in the northern Indian Ocean [*Goyet et al.*, 1999]. In the deep waters at the equatorial Indian Ocean and the southern Bay of Bengal the measured Δ^{14}C values below 2500 m are higher than the estimated pre-nuclear Δ^{14}C profile (derived from silica) by about 20‰. Presence of Antarctic bottom water with higher silica content at these depths causes this deviation. The

Table 1. Inventory and Mean Penetration Depths of Bomb-^{14}C, and Bomb-^{14}C Based Air-Sea CO_2 Exchange Rates in the Northern Indian Ocean[a]

Station	Location (Lat °N; Long. °E)	Sampling Time (month/year)	Surface Δ^{14}C (‰)	Surface $\Delta\Delta^{14}$C (‰)	Mean Penetration Depth[a] (m)		Specific Bomb-^{14}C Inventory (10^9 atoms cm^{-2})		Air-Sea CO_2 Exchange Rates F_{12} (mol m^{-2} yr^{-1})	
					A	*B*	*A*	*B*	*A*	*B*
Arabian Sea										
GEOSECS 413	13.35; 53.27	Dec 1977	72	142	333	—	7.3	—	17.9	—
GEOSECS 416	19.75; 64.62	-do-	59	139	284	297	6.3	6.2	15.4	13.9
GEOSECS 417	12.97; 64.47	Jan 1978	75	145	231	220	5.2	5.0	12.7	11.0
GEOSECS 418	6.18; 64.42	-do-	75	135	293	269	6.1	6.0	15.0	13.7
GEOSECS 419	3.95; 56.80	-do-	95	155	207	—	4.8	—	11.8	—
SS118-E-8	15.30; 71.50	Mar 1994	31	101	225	218	3.5	3.5	7.5	7.0
SS118-F-6	17.90; 70.30	-do-	37	117	286	302	5.2	5.2	11.1	10.4
SS118-H-12	19.75; 64.62	-do-	33	113	318	337	5.9	5.9	12.6	11.8
SS132–3269	12.80; 71.60	Apr 1995	57	110	275	287	4.8	5.1	10.3	10.4
SS132–3271	12.97; 64.47	-do-	57	127	337	321	6.9	6.6	14.8	13.2
SS132–3272	13.20; 58.30	May 1995	41	111	369	329	6.4	5.8	13.7	11.7
SS132–3273	5.70; 56.20	-do-	55	115	441	387	8.0	7.7	17.1	16.0
SS132–3274	6.18; 64.42	-do-	58	118	346	314	6.4	6.3	13.7	12.4
SS132–3275	8.00; 74.00	-do-	56	127	253	250	5.0	5.0	10.7	10.2
SS164–4018	13.35; 53.27	Apr 1998	43(75 m)	110	461	—	8.0	—	17.2	—
Bay of Bengal										
GEOSECS 445	8.50; 86.02	Mar 1978	102	162	153	—	3.7	—	9.0	—
GEOSECS 446	12.50; 84.50	-do-	117	172	183	—	4.5	—	10.9	—
GEOSECS 448	0.00; 80.10	-do-	113	173	194	—	5.0	—	12.1	—
SS152–3829	8.30; 86.02	Feb 1997	38	98	360	—	5.5	—	11.8	—
SS152–3846	0.00; 80.00	-do-	55	115	533	—	9.5	—	20.4	—
SS172–4030	18.98; 89.53	Feb 1999	18	68	299	—	3.1	—	6.7	—
SS172–4036	13.06; 94.09	-do-	44	99	280	—	4.2	—	9.1	—
SS172–4037	10.80; 94.76	-do-	40	95	296	—	4.3	—	9.3	—
SS172–4041	5.00; 86.00	-do-	57	117	250	—	4.5	—	9.7	—

[a]A: Values determined in this work. B: As reported in *Bhushan et al.* [2000].

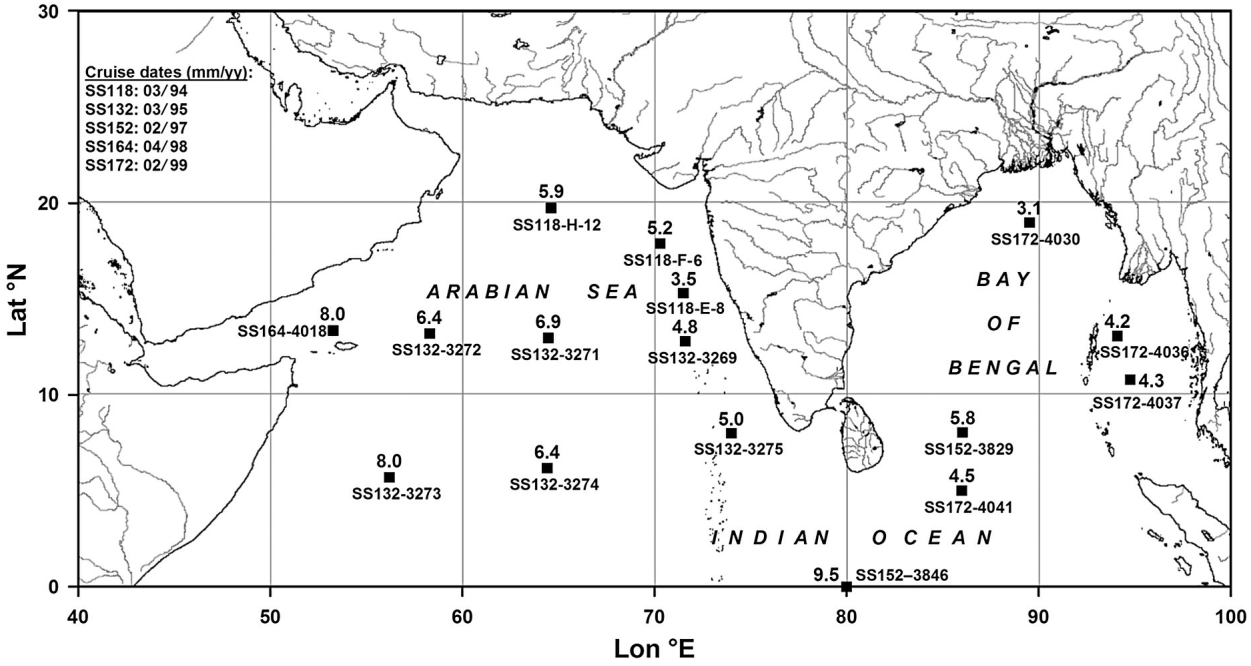

Figure 5. Bomb-^{14}C inventories ($\times 10^9$ atoms cm^{-2}) for the stations occupied between 1994 and 1999.

scatterplot of Δ^{14}C versus silica for global ocean waters deeper than 1000 m [*Broecker et al.*, 1995] shows significant deviation from the linearity at the high silica end caused by circum-polar waters. However, this feature is not seen in the southern Bay of Bengal station SS172–4041.

3.1. Inventories of Bomb-^{14}C in the Northern Indian Ocean

[14] The inventories and mean penetration depths of bomb ^{14}C were determined from the column-integrated bomb-^{14}C, ΣCO_2 and the surface ^{14}C excess, following the procedures outlined in *Broecker et al.* [1985] (Appendix B). The inventories for the GEOSECS stations and for the Arabian Sea stations occupied during 1994 and 1995 [*Bhushan et al.*, 2000] are recalculated using the pre-nuclear surface ocean Δ^{14}C values (Appendix A). The results are shown in Table 1. No significant changes are noticed in the recalculated values of bomb-^{14}C inventories and mean penetration depths, from the values reported in *Bhushan et al.* [2000].

[15] The snapshot distributions of bomb-^{14}C in the northern Indian Ocean as observed during 1977–1978 (GEOSECS) [*Stuiver and Östlund*, 1983], during 1994–1995 [*Somayajulu et al.*, 1999; *Bhushan et al.*, 2000] and during 1997–1999 are shown in Figures 4 and 5. Between 1977 and 1978 and late 1990s the bomb-^{14}C inventories has increased up to 10% on the average for most stations in the northern Indian Ocean, excluding the stations near the equatorial Indian Ocean, e.g., SS132–3273 (near GEOSECS 419) and SS152–3846 (reoccupation of GEOSECS 448), where bomb-^{14}C inventory has increased by ∼80% (Table 2). The mean ^{14}C penetration depths also have been more than doubled at these stations. In the equatorial Indian Ocean station SS152–3846, the largest increase of bomb-^{14}C has been observed for depths between 200 m and 1000 m (Figure 3). Major portion of this bomb-^{14}C were seen above 500 m. From the reoccupation of GEOSECS equatorial Indian Ocean stations (between 4°N and 6°S) during the French INDIGO expeditions of 1981–1987, it has been shown that bomb-^{14}C inventory had increased to ∼90% and the penetration depth had increased to ∼80% [*Bard et al.*, 1988, 1989]. This increase has been attributed to the westward flowing waters with high concentration of bomb tracers, due to the entry of ^{14}C-enriched Pacific waters through the passages in the Indonesian archipelago, or mixing with the Mode water from the southern gyre of the Indian Ocean. Evidence of influx of Pacific water through the Indonesian archipelago has been demonstrated from GEOSECS surface tritium distribution [*Fine*, 1985], and high concentration of ^{90}Sr in banded corals from the western Indian Ocean [*Toggweiler and Trumbore*, 1985]. *Povinec et al.* [2010] observed that concentrations of tritium, ^{14}C, ^{90}Sr, and ^{129}I in the surface waters of the Indian Ocean were similar to that of the northwestern Pacific Ocean, and attributed them to transport of Pacific Ocean water masses to the Indian Ocean through the Indonesian Seas. Such lateral transport processes must have been operative for the observed large increase in bomb-^{14}C inventories at the stations SS132–3273 and SS152–3846. The inventory at SS172–4041 (near GEOSECS 445) which doesn't fall in the path of the

Table 2. Changes in Bomb-^{14}C Inventories in Two Decades Since GEOSECS

Stations: GEOSECS/ PRL Reoccupied	Bomb-^{14}C Inventory ($\times 10^9$ atoms cm^{-2})		
	GEOSECS (1977–1978)	PRL Expeditions (1994–1999)	Inventory Change in Two Decades
GEOSECS-413/SS164–4018	7.3	8.0	0.7
GEOSECS-416/SS118-H-12	6.3	5.9	−0.4
GEOSECS-417/SS132–3271	5.2	6.9	1.7
GEOSECS-418/SS132–3274	6.1	6.4	0.3
GEOSECS-419/SS132–3273	4.8	8.0	3.2
GEOSECS-445/SS152–3829	3.7	5.5	1.8
GEOSECS-448/SS152–3846	5.0	9.5	4.5

throughflow water for its NW–SE trend, has not changed much since 1978, although it is at the same latitude (5°N) as SS132–3273. Lowest ^{14}C inventory obtained for the station SS172–4030 (3.1×10^9 atoms cm^{-2}), about 25% lower than other contemporary Bay of Bengal values.

3.2. Comparison of Observed Changes of Bomb-^{14}C Inventories With Modeled Values

[16] *Toggweiler et al.* [1989] simulated the penetration of bomb-produced ^{14}C in the world ocean using the Geophysical Fluid Dynamics Laboratory's (GFDL) primitive equation ocean general circulation model. Changes in the inventories of bomb-^{14}C have been simulated using this model, for the entire world ocean. In this study the comparison of changes in bomb-^{14}C inventories are done between 1970s and late 1990s, the predicted changes between 1990 and 1981 should be considered as the lower limit. For the decade 1981 to 1990, the model predicts increase in bomb-^{14}C inventories from 0 to 2×10^9 atoms cm^{-2} for the Arabian Sea and the equatorial Indian Ocean, while no change has been predicted for the Bay of Bengal. The average bomb-^{14}C inventory for the GEOSECS stations 416, 417 and 418 during 1977 was 5.9×10^9 atoms cm^{-2}, which rose to 6.4×10^9 atoms cm^{-2} during 1994 and 1995. Average bomb-^{14}C inventory in the Bay of Bengal during 1978 was 4.1×10^9 atoms cm^{-2}; while during 1997 and 1999 it rose to 4.4×10^9 atoms cm^{-2}, consistent with the model prediction. Major discrepancy is seen at the equatorial Indian Ocean, where the inventory increased by 4.5×10^9 atoms cm^{-2} between 1978 and 1997, which is more than twice the model predicted rise between 1981 and 1990. Thus, the observed ^{14}C values in the northern Indian Ocean obtained from this work and from *Bhushan et al.* [2000] agrees with the GFDL model simulated values, except at the equatorial Indian Ocean. *Peacock* [2004] based on model based calculations projected roughly 30% increase in ocean bomb radiocarbon inventory between the mid-1970s and mid-1990s.

3.3. Changes in Penetration Depths of Bomb-^{14}C in the Northern Indian Ocean

[17] The average value of the mean penetration depth during 1977–1978 for the five Arabian Sea GEOSECS stations (413, 416, 417, 418 and 419) was 270 m (Table 1). During 1994–1998, this has increased by ~40%, to 381 m on the average (considering only the reoccupation or nearby stations). In the Bay of Bengal, the mean penetration depth has increased by ~80%, from 168 m in 1978 (for the two GEOSECS stations 445 and 446), to 297 m during 1997 and 1999 (average of five stations). The relative increase of mean penetration depths in two decades is higher for the Bay of Bengal than that for the Arabian Sea, although the actual depth of penetration of bomb-^{14}C is always higher in the Arabian Sea than in the Bay of Bengal. This could be due slower rate of penetration of bomb-^{14}C in the Bay of Bengal during the GEOSECS times, when due to strong isopycnal gradient, bomb-^{14}C was mainly accumulated within the top ~200 m of water column. This also explains higher surface $\Delta^{14}C$ in the Bay of Bengal than in the Arabian Sea during the GEOSECS. The downward transfer of bomb-^{14}C would have become faster after it crossed the surface barrier of isopycnal gradient, thus causing relatively large increase in the penetration depths of bomb-^{14}C after GEOSECS. However, since mean penetration depth is inversely proportional to the change in the surface ocean $\Delta^{14}C$ from the pre-nuclear values (Appendix B), and the latter is steadily falling due to continuously decreasing atmospheric $\Delta^{14}C$, the observed changes in the mean penetration depths can also be explained from changes in the surface $\Delta^{14}C$ values. From subsequent ^{14}C measurements in the northern Indian Ocean, *Dutta et al.* [2010] showed that the decline of $\Delta^{14}C$ in the surface Bay of Bengal was just ~4‰ in one decade between 1995 and 2006, as compared to ~25‰ observed in two decades between 1978 and 1995. The smaller rates of surface ocean $\Delta^{14}C$ decline in the recent decades can be attributed to much smaller decrease-rate of ~5‰ yr^{-1} of the atmospheric $\Delta^{14}C$ during late-1990s [*Dutta et al.*, 2006], as compared to ~12‰ yr^{-1} between 1978 and 1995 [*Hua and Barbetti*, 2004].

4. ^{14}C-based Air-Sea CO_2 Exchange Rates in the Northern Indian Ocean

[18] Air-sea exchange rates of CO_2 have been calculated for all stations based on the bomb ^{14}C inventories following the procedure of *Stuiver* [1980], as described in Appendix B. The method is based on the assumption, that the net amount of bomb-^{14}C gone into the ocean is proportional to the integrated atmosphere-ocean $\Delta^{14}C$ gradient and the regional air-sea exchange rate of CO_2. Another assumption of this procedure is that the changes in the bomb-^{14}C inventory only result from air-sea exchange of CO_2 and vertical diffusive mixing, and the invasion of CO_2 from air to sea is equal to its evasion out of the sea. However, this assumption may not be valid for some locations, e.g., SS172–4030 and SS152–3846 where lateral transport plays a significant role in deciding the bomb-^{14}C inventory. To ascertain and quantify the component of bomb-^{14}C contribution due to lateral transport, detailed measurements of ^{14}C profiles are needed with better vertical and spatial coverage.

4.1. Distribution of Air-Sea CO_2 Exchange Rates Over the Northern Indian Ocean

[19] *Bhushan et al.* [2000] had reported the air-sea CO_2 exchange rates for the Arabian Sea from the GEOSECS ^{14}C measurements and from the measurements made during 1994 and 1995. In that study, tropospheric $\Delta^{14}C$ history for the northern hemisphere was used, which has peak $\Delta^{14}C$ of ~1000‰ in 1964 [*Bhushan et al.*, 1997]. As far as tropical Indian Ocean is concerned, it is more appropriate to use the tropospheric $\Delta^{14}C$ trend for the Northern Hemisphere Zone 3 as discussed in *Hua and Barbetti* [2004], where the peak $\Delta^{14}C$ was ~700‰ in 1965. *Chakraborty et al.* [2008] reported peak tropospheric $\Delta^{14}C$ of 708 ± 8‰ from tree rings of central India grown in 1965. In this study we have adopted a peak $\Delta^{14}C$ of 700‰. In *Bhushan et al.* [2000] the mixed layer $\Delta^{14}C$ trend was derived from a Gulf of Kutch coral, which recorded peak $\Delta^{14}C$ of 170‰ in 1968 [*Chakraborty et al.*, 1994]. The mixed-layer $\Delta^{14}C$ trend recorded in the Gulf of Kutch may not be representative for the open northern Indian Ocean. If the $\Delta^{14}C$ trend from the Gulf of Kutch coral is used then, the integrated mixed-layer $\Delta^{14}C$ value would be an overestimate, due to the overall higher $\Delta^{14}C$ values in the Gulf of Kutch than the contemporary open northern Indian Ocean waters. However, since

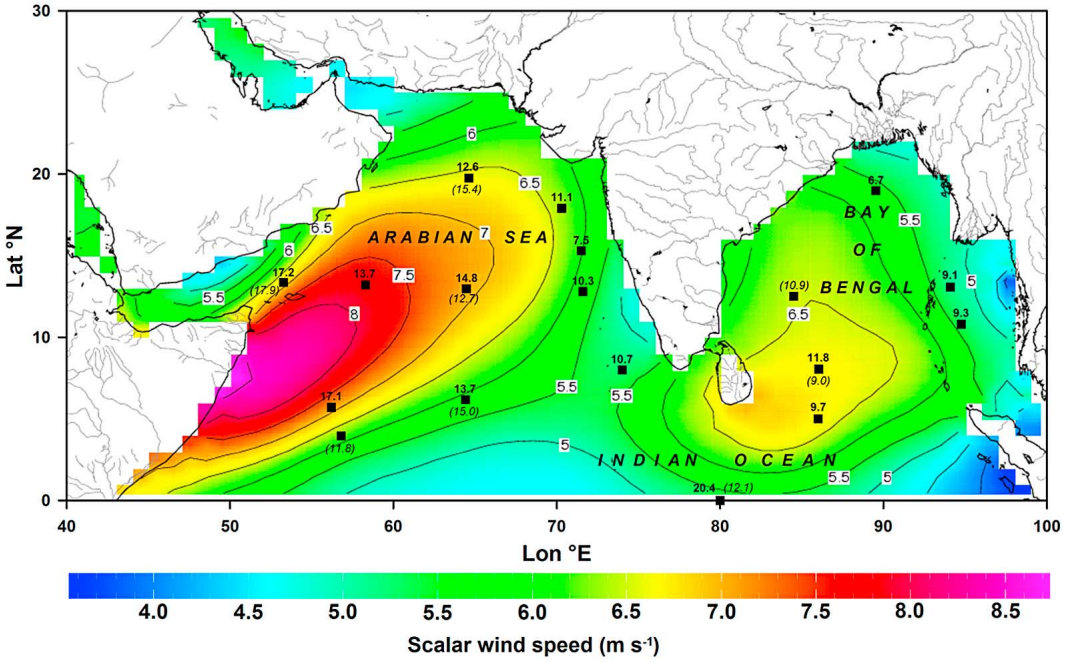

Figure 6. Contours of long-term mean surface scalar wind speeds (m s^{-1}) over northern Indian Ocean [*da Silva et al.*, 1994], and bomb-^{14}C based air-sea CO_2 exchange rates (mol m^{-2} yr^{-1}) for the measurements done between 1994 and 1999. Values in parentheses are the exchange rates calculated from GEOSECS ^{14}C data. Climatology wind speed contour map created from IRI/LDEO Climate Data Library at http://iridl.ldeo.columbia.edu.

for determining the ^{14}C input, it is the atmosphere-ocean gradient of Δ^{14}C that is integrated, the effect of using higher Δ^{14}C values for both the atmosphere and the ocean mixed layer is likely to cancel each other. The ^{14}C based air-sea CO_2 exchange rates for the northern Indian Ocean stations are given in Table 1. As compared to the values reported in *Bhushan et al.* [2000], the exchange rates recalculated in this study are higher by ~9% on an average for all but one station in the Arabian Sea (the recalculated values are higher by −1 to 17% for different stations).

[20] The air-sea CO_2 exchange rates in the northern Indian Ocean calculated from the bomb-^{14}C inventories range from ~7 mol m^{-2} yr^{-1} (in the northern Bay of Bengal) to 20 mol m^{-2} yr^{-1} (in the equatorial Indian Ocean). High CO_2 exchange rates of ~17 mol m^{-2} yr^{-1} are measured in the western Arabian Sea, off Oman and near the Gulf of Aden (Table 1 and Figure 6). The high exchange rate obtained at the equator (and also possibly at SS132–3273) could be an artifact of lateral advection of ^{14}C-enriched waters from the Pacific into this area from the Indonesian archipelago.

[21] The measured air-sea CO_2 exchange rates are plotted with the long-term wind speed in Figure 7. All points for the northern Indian Ocean station fall on a roughly linear trend, for wind speeds ranging from 5 to 8 m sec^{-1}. From the GEOSECS ^{14}C measurements, *Broecker et al.* [1985] determined mean exchange rate of 20 mol m^{-2} yr^{-1} for the global ocean, using global average surface wind speed of 7.4 m sec^{-1}. From ^{14}C measurements in corals from the Red Sea, an invasion flux of 8 ± 2 mol m^{-2} yr^{-1} has been obtained, for a mean wind speed 4.7 m sec^{-1} [*Cember*, 1989]. As expected, the CO_2 exchange rates calculated from the Red Sea coral, northern Indian Ocean measurements from this study and the global mean value obtained from GEOSECS ^{14}C data [*Broecker et al.*, 1985], follow a rough trend. Also shown in Figure 7 are the empirical linear, quadratic and cubic relationships established between long-term average wind speed and CO_2 exchange rates [*Wanninkhof et al.*, 1985; *Wanninkhof*, 1992; *Wanninkhof and McGillis*, 1999; *Sweeney et al.*, 2007]. The cubic relationship appears to fit better with the bomb-^{14}C derived CO_2 exchange rates in the northern Indian Ocean.

[22] In Figure 7, the exchange rate obtained for the equatorial Indian Ocean station SS152–3846 during 1997, is a clear outlier from the general polynomial trend. It is interesting to note here, that using the bomb-^{14}C inventory measured at this station during 1978 (GEOSECS 448) and the local long-term wind speed of ~5 m sec^{-1}, one gets an exchange rate of 12.1 mol m^{-2} yr^{-1}, which fits better with the general trend. As discussed, significant change in bomb-^{14}C at this location is due to lateral advection of waters from the Pacific. Assuming lateral advection a steady state process, the fact that the inventory of GEOSECS 448 matches the regional wind speed indicates that the Δ^{14}C of the water that is flowing in to this region has steadily increased in the last two decades since 1978. This increase is in response to the bomb transient, with a delay introduced by the transport processes. Thus, in the equatorial Indian Ocean, between 1978 and 1997, a major portion of the increment in the bomb-^{14}C inventory is through lateral advection of ^{14}C-enriched waters, rather than through air-sea CO_2 exchange. The combined effects of uncertainties in the gas transfer velocity and wind fields lead to average difference of 27% between the lowest and highest estimates of the CO_2 flux from the region [*Feely et al.*, 2004].

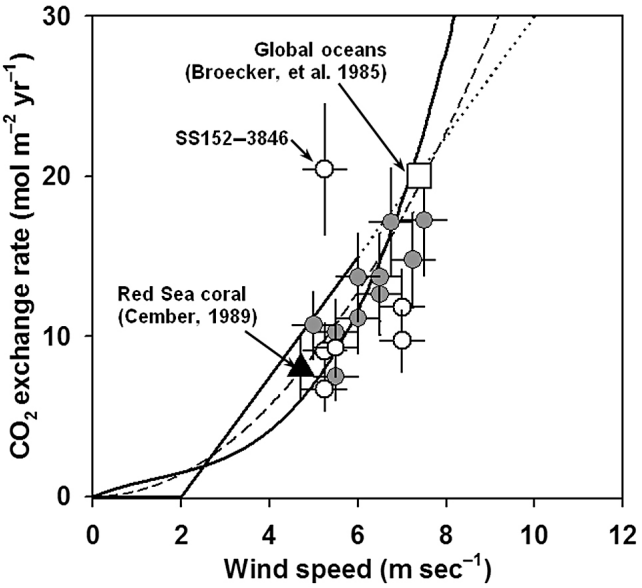

Figure 7. Dependence of ^{14}C derived CO_2 exchange rates with long-term mean scalar wind speed. The filled and open circles denote bomb-^{14}C based exchange rates measured at the Arabian Sea and the Bay of Bengal stations respectively, between 1994 and 1999. The open square is the global average CO_2 exchange rate from GEOSECS ^{14}C measurements [*Broecker et al.*, 1985]. The filled triangle is the value obtained from ^{14}C in Red Sea coral [*Cember*, 1989]. The CO_2 exchange rates are obtained from the gas transfer rates from the CO_2 solubility function of *Weiss* [1974]. The gas transfer rates are calculated from the empirical relationships with wind speed and are shown by (i) solid straight line extrapolated with dotted line (SF_6 experiment in lake [*Wanninkhof et al.*, 1985]), (ii) dashed curved line (quadratic relationship for long-term average winds [*Wanninkhof*, 1992]) and (iii) solid curved line (cubic relationship for long-term average winds [*Wanninkhof and McGillis*, 1999].

4.2. Estimate of Net Sea-Air Flux of CO_2 From the Northern Indian Ocean

[23] Both in the Arabian Sea and the Bay of Bengal, large seasonal variations of pCO_2 in the surface waters are seen due to strong seasonality of wind induced upwelling and nutrient inputs through large amount of river discharge [*Kumar et al.*, 1992]. Throughout the year surface pCO_2 for the Arabian Sea is higher than in the Bay of Bengal [*Sarma et al.*, 1998], which increases during the southwest monsoon season [*Körtzinger et al.*, 1997].

[24] We have divided the northern Indian Ocean region into four regions: (i) Arabian Sea (6°N to 25°N and 40°E to 80°E, including Red Sea mouth, and excluding Persian Gulf); (ii) North Bay of Bengal (14°N to 22°N and 80°E to 97°E); (iii) South Bay of Bengal (6°N to 14°N and 80°E to 100°E); and (iv) North Tropical Indian Ocean (2°S to 6°N and 41°E to 100°E). The average ΔpCO_2 and air-sea CO_2 exchange rates were interpolated for each of these regions in $4° \times 5°$ grids, using the gridded ΔpCO_2 values of *Takahashi et al.* [2009]. The net CO_2 fluxes from these northern Indian Ocean regions were calculated from the regional average exchange rates and the ocean-atmosphere pCO_2 gradients (ΔpCO_2). We have used atmospheric pCO_2 of 356 μatm, as mean difference of pCO_2 of seawater and ΔpCO_2 reported in *Takahashi et al.* [2009]. The results are summarized in Table 3 and Figure 8.

[25] We estimate net annual flux of CO_2 from the northern Indian Ocean region (between 0° to 25°N) to $\sim 104 \pm 30$ Tg C yr^{-1}. The source of this flux is entirely located in the Arabian Sea, with annual sea-air flux of $\sim 69 \pm 21$ Tg C yr^{-1}. The Bay of Bengal as a whole is a sink of atmospheric CO_2, where the sink is mainly located in its northern part. The estimated net uptake rate of CO_2 by the Bay of Bengal is $\sim 1 \pm 0.4$ Tg C yr^{-1}. The CO_2 source in the tropical Indian Ocean within 0° and 6°N is estimated to $\sim 35 \pm 11$ Tg C yr^{-1}. Our estimated sea-air fluxes agree well with the values reported in *Takahashi et al.* [2009], where the flux from the temperate Indian Ocean (north of 14°N) has been estimated to 0.02 Pg C yr^{-1}, and 0.1 Pg C yr^{-1} for the tropical Indian Ocean between 14°S and 14°N. *Bates et al.* [2006] based on wind speed based exchange rates determined net sea-to-air CO_2 flux of 237 ± 132 Tg C yr^{-1} for the Indian Ocean and found that the Arabian Sea, Bay of Bengal, and 10°N–10°S zones were perennial sources of CO_2 to the atmosphere, although the Bay of Bengal became a sink for CO_2 in December. *Louanchi et al.* [1996] estimated annual flux of 169 TgC yr^{-1} for the northern Indian Ocean between 10°S and 18°N, using a one-dimensional model and incorporating the effects of physical and biogeochemical processes. *Gruber et al.* [2009] based on the model calculations of estimates of the contemporary net air-sea CO_2 fluxes, showed a consistent description of the regional distribution of annual mean sources and sinks of atmospheric CO_2 for the decade of the 1990s and the early 2000s. They found that this distribution is characterized by outgassing in the tropics, uptake in midlatitudes, and comparatively small fluxes in the high latitudes. However, to constrain the derived estimates in the Arabian Sea and the Bay of Bengal, more detailed measurements of radiocarbon in the water column and surface ocean pCO_2 in the Arabian Sea and the Bay of Bengal

Table 3. Estimates of Sea to Air Flux of CO_2 for the Northern Indian Ocean

Region	Approx. Area (10^6 km^2)	Mean ΔpCO_2 (μatm)	Mean Air-Sea CO_2 Exchange Rate (mol m^{-2} yr^{-1})	Mean CO_2 Flux Rate (mol m^{-2} yr^{-1})	Net Regional Flux of CO_2 (Tg C yr^{-1})
Arabian Sea (6°–25°N, 50°E–80°E)	4.83	+30.3	14 ± 3	+1.3	$+69 \pm 21$
North Bay of Bengal (14°N–22°N, 80°E–97°E)	1.03	−8.7	7 ± 1	−0.2	-2.1 ± 0.6
South Bay of Bengal (6°N–14°N, 80°E–100°E)	1.63	+2.3	9 ± 2	+0.1	$+1.5 \pm 0.5$
North Tropical Indian Ocean (2°S–6°N, 45°E–95°E)	5.24	18.1	14 ± 3	+0.8	$+49 \pm 15$

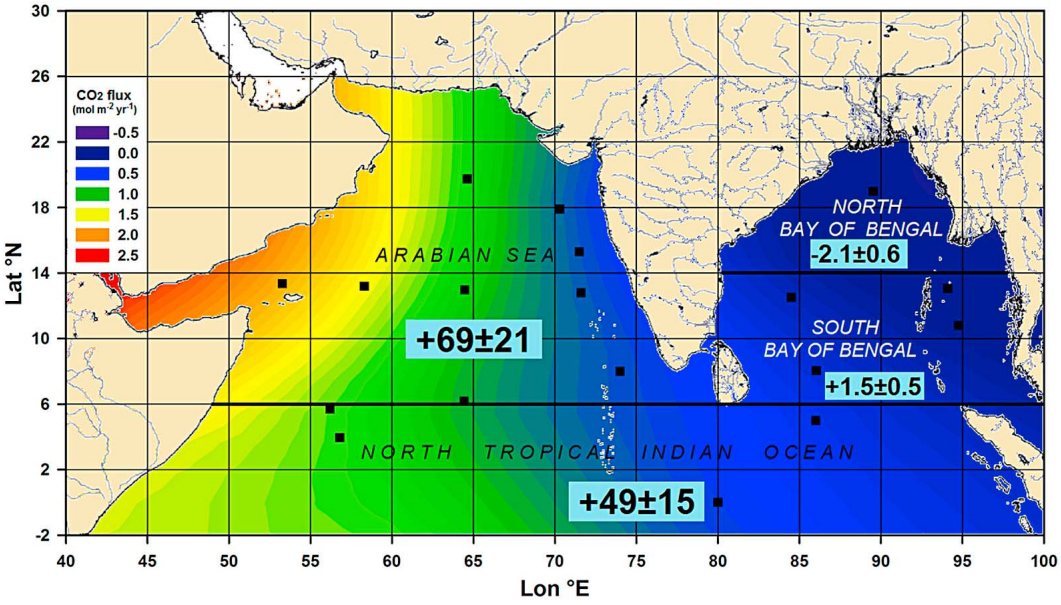

Figure 8. Contours of sea-air flux of CO_2 in the northern Indian Ocean. Net regional CO_2 fluxes (in Tg C yr^{-1}) are shown in the boxes for the four regions. Positive values of flux indicate net source (as in the Arabian Sea and the North Tropical Indian Ocean), while negative flux indicates net sink (as for the North Bay of Bengal).

with more spatial and temporal variability are required to constrain the CO_2 invasion and evasion rates.

5. Conclusion

[26] This study reports the changes in the distribution of ^{14}C in the water column of the Bay of Bengal, the equatorial Indian Ocean and near the Red Sea mouth, about two decades after the GEOSECS expedition. Our measurements show on an average there was only marginal change in the inventory of nuclear-bomb produced ^{14}C in the Arabian Sea and the Bay of Bengal, in two decades between 1978 and 1999. The bomb-^{14}C inventory has nearly doubled to 9.5×10^9 atoms m^{-2} in the equatorial Indian Ocean, likely due to lateral advection of ^{14}C rich waters from the southeast. The air-sea CO_2 exchange rates based on bomb-^{14}C inventories range from 7 to 17 mol m^{-2} yr^{-1}. Except for the equatorial Indian Ocean, the ^{14}C-derived exchange rates are mostly a function of long-term wind speeds over this region. From the average ^{14}C derived CO_2 exchange rates and reported annual surface seawater pCO_2 values, the net flux of CO_2 from the Indian Ocean in the late 1990s has been estimated to $\sim 104 \pm 30$ TgC yr^{-1}.

Appendix A: Reconstruction of Pre-nuclear $\Delta^{14}C$ Profiles

[27] To assess the temporal changes of bomb-^{14}C, data on the steady state or pre-nuclear $\Delta^{14}C$ profiles are required. In the absence of the measurements of pre-nuclear $\Delta^{14}C$ profiles, they can be reconstructed based on the pre-nuclear surface $\Delta^{14}C$ (derived from marine mollusk shells of known age) and the profiles of bomb produced tritium (^3H) or dissolved silicate [*Broecker et al.*, 1985, 1995]. In this work, the pre-nuclear $\Delta^{14}C$ profiles for different stations are reconstructed from the measured silicate data, based on the empirical linear relationship for the global ocean between the natural $\Delta^{14}C$ and silicate ($\Delta^{14}C_{natural} = -70 -$ silicate), established by *Broecker et al.* [1995], where $\Delta^{14}C$ is expressed in permil (‰) and Silicate in micromole per kg (μmol kg^{-1}). The above linear relationship has been derived from the $\Delta^{14}C$-silicate data of GEOSECS samples deeper than 1000 m, which are uncontaminated with bomb-^{14}C and ^3H. Deep waters originating from Antarctic circum-polar regions have relatively higher $\Delta^{14}C$ and therefore deviate from the above linear relationship. From the GEOSECS deep-water samples of the Arabian Sea and the Bay of Bengal with Silicate >50 μmol kg^{-1}, *Bhushan et al.* [2000] obtained a relation $\Delta^{14}C_{natural} = -80 - 0.83$*silicate. The pre-nuclear $\Delta^{14}C$ profiles based on this relation and those derived from *Broecker et al.* [1995] are consistent within ±10‰. The estimated uncertainty of reconstructing the pre-nuclear $\Delta^{14}C$ using the linear relation of *Broecker et al.* [1995] is also ±10‰ [*Peng et al.*, 1998]. Therefore, reconstruction of pre-nuclear $\Delta^{14}C$ for the northern Indian Ocean using the relation ($\Delta^{14}C_{natural} = -80 - 0.83$*silicate) will not be significantly different from that derived using the relation of *Broecker et al.* [1995]. In this study, the pre-nuclear profiles have been calculated from the relation ($\Delta^{14}C_{natural} = -70 -$ silicate). *Rubin and Key* [2002] developed a new separation method based on the strong linear correlation between $\Delta^{14}C$ and potential alkalinity. This method provides an estimate of surface ocean pre-bomb $\Delta^{14}C$ concentrations. However, this method is not applicable to all regions. The primary disadvantage relative to the silicate method is that high quality alkalinity measurements are less common than high quality silicate measurements. For low- and midlatitude waters, both methods give comparable results and for high latitude southern

Table A1. Pre-nuclear Surface $\Delta^{14}C$ Values Adopted for the Northern Indian Ocean[a]

Region	Surface $\Delta^{14}C_{natural}$
Northern Bay of Bengal (*Chilika Lake*)	−50‰
Central Bay of Bengal and Andaman Sea (*Stewart Sd.*)	−55‰
Southern Bay of Bengal (*Rameswaram*)	−60‰
Equatorial Indian Ocean (*Rameswaram*)	−60‰
Southern Arabian Sea (*Rameswaram*)	−60‰
Central Arabian Sea (*Bombay, Goa and Malabar*)	−70‰
Northern Arabian Sea (*Dwarka and Port Okha*)	−80‰

[a]All values are after *Dutta et al.* [2001], except for the Central Arabian Sea data which is from *Southon et al.* [2002].

waters, the potential alkalinity method predicts lower natural $\Delta^{14}C$ and consequently higher bomb ^{14}C.

[28] The pre-nuclear surface $\Delta^{14}C$ values used in this study for different regions are based on the $\Delta^{14}C$ measurements of pre-nuclear shells [*Dutta et al.*, 2001; *Southon et al.*, 2002], rounded off to nearest 10‰. The surface Silicate values are adjusted to match the reconstructed pre-nuclear surface $\Delta^{14}C$ with the values estimated from shells. The pre-nuclear surface $\Delta^{14}C$ values adopted for different regions of the northern Indian Ocean are given in Table A1.

Appendix B: Determination of Bomb-^{14}C Inventories and Air-Sea CO_2 Exchange Rates

[29] The inventories of bomb-^{14}C are calculated following the procedures of *Broecker et al.* [1985]. The area (A) between the measured $\Delta^{14}C$ depth profile and the reconstructed pre-nuclear $\Delta^{14}C$ depth profile ($\Delta^{14}C^0$) is calculated as

$$A = \int_0^{z^0} \left(\Delta^{14}C - \Delta^{14}C^0\right) dz \quad \text{(B1)}$$

Here, z^0 is the depth at which the difference between $\Delta^{14}C$ and $\Delta^{14}C^0$ becomes negligible (<1‰). The mean penetration depth (Z) of bomb-^{14}C is obtained as

$$Z = A/\left(\Delta\Delta^{14}C\right) \quad \text{(B2)}$$

Here, $\Delta\Delta^{14}C = (\Delta^{14}C - \Delta^{14}C^0)_{surface}$ is the measured excess of surface water $\Delta^{14}C$ from its pre-nuclear value. The total column-inventory of bomb-^{14}C is given by

$$\Sigma^{14}C = \Sigma CO_2 \times A \times k \quad \text{(B3)}$$

Here ΣCO_2 is the mean DIC of the water column up to which bomb-^{14}C has penetrated. The proportionality constant 'k' takes into account density of seawater (average ~1025 kg m^{-3}), Avogadro's number (6.023×10^{23} atoms mol^{-1}), and the $^{14}C/^{12}C$ atom ratio of the NBS Oxalic Acid-I standard (1.176×10^{12} [*Karlen et al.*, 1968]). The inventory of bomb-^{14}C is expressed in units of atoms of ^{14}C per square unit area of the seawater column. Following this procedure, the estimate uncertainty of the calculated inventory is about ±10% [*Peng et al.*, 1998]. To compute the bomb-^{14}C inventories, the measured depth profiles of $\Delta^{14}C$, silicate and ΣCO_2 values were interpolated to every 1 m. Pre-nuclear $\Delta^{14}C$ profiles ($\Delta^{14}C^0$) were then reconstructed from the measured values of silicate, using the empirical relationship of *Broecker et al.* [1995], $\Delta^{14}C^0$ (‰) = −70 − silicate (μmol kg^{-1}). The reconstructed pre-nuclear $\Delta^{14}C$ of surface was forced to match with the values obtained from pre-bomb shells. The excess (measured $\Delta^{14}C$ − $\Delta^{14}C^0$) are then integrated until the difference becomes negligible and the inventory of bomb-^{14}C is obtained using (B1) and (B3).

[30] The air-sea CO_2 exchange rates were calculated following the procedure outlined by *Stuiver* [1980] The total amount of bomb-^{14}C penetrated in ocean is proportional to the air-sea exchange rate of CO_2 and the time integrated gradient of $\Delta^{14}C$ between the atmosphere ($\Delta^{14}C_{atm}$) and the ocean surface mixed layer ($\Delta^{14}C_{mix}$). Assuming the mean steady state difference in $\Delta^{14}C$ values between atmosphere and oceanic mixed layer is −60‰ for the northern Indian Ocean, the total amount of bomb-^{14}C (Q_{14}), transferred per unit of ocean surface over time t (in years) is related to the air-sea exchange rate of CO_2 (F_{12}) as

$$Q_{14} = 1.24 \times 10^{-15} F_{12} \int_0^t \left(\Delta^{14}C_{atm} - \Delta^{14}C_{mix} - 60\right) dt \quad \text{(B4)}$$

The constant term on the right hand side of (B4), takes into account the isotopic fractionation factors for ocean-atmosphere transfer and normalization of ^{14}C activity to $\delta^{13}C$ value of −25‰ [*Stuiver*, 1980]. Here Q_{14} is expressed in mol m^{-2} and F_{12} in mol m^{-2} yr^{-1}. For the onset of input of bomb-^{14}C to the oceans, 1954 is taken as the initial year ($t = 0$). The values of the integrals for $\Delta^{14}C_{atm}$ and $\Delta^{14}C_{mix}$ are obtained from $\Delta^{14}C$ measurements in the atmosphere and in corals. The tropospheric $\Delta^{14}C$ from 1954 and 1968 has been adopted from the reported measurements from the tropical regions [*Nydal and Lövseth*, 1996; *Hua and Barbetti*, 2004; *Chakraborty et al.*, 2008], with peak $\Delta^{14}C$ of 700‰ in the year 1965. From 1968 onward, an exponentially decreasing atmospheric $\Delta^{14}C$ trend with e-folding time of 17 years has been adopted, fixing the $\Delta^{14}C$ for the years 1980 and 1999 at 265‰ and 88‰ respectively. There are too few coral $\Delta^{14}C$ measurements in the open northern Indian Ocean, to reconstruct the mixed layer $\Delta^{14}C$ history for different regions. Between the years 1954 and 1973, the value of the integral of $\Delta^{14}C_{mix}$ is taken as 1400 [*Stuiver*, 1980]. From 1973 onward, a linear decrease of surface ocean $\Delta^{14}C$ has been assumed, from a value of 140‰ in 1973 to 50‰ in 2000, to match with the observed values from the GEOSECS measurements during 1977–1978 [*Stuiver and Östlund*, 1983] and during late 1990s [*Dutta et al.*, 2006]. Q_{14} are calculated from the bomb ^{14}C inventories for different stations, to determine the air-sea CO_2 exchange rates (F_{12}) using (B4). Based on the uncertainty in bomb-^{14}C inventory (15%) and the integral of the atmosphere-ocean $\Delta^{14}C$ gradient (5%), the uncertainty of ^{14}C-based exchange rates estimated to ~20%. *Druffel and Griffin* [2008] showed that for surface samples, the total uncertainty of a DIC $\Delta^{14}C$ value at a given site over a several week period is approximately two times the reported uncertainty (~7‰). Thus, depending on the

application, post-bomb $\Delta^{14}C$ data should consider this short-term variability of surface ocean $\Delta^{14}C$ values and factor this into their analysis as it might affect the estimates of air-sea CO_2 exchange rates.

[31] Once the rate of air-sea CO_2 exchange (F_{12}) is known, the net transfer rate (F) of atmospheric CO_2 across the ocean surface can be determined from the difference of the partial pressure of CO_2 (ΔpCO_2) in the surface ocean and that in the atmosphere [*Wanninkhof*, 1992]. The net transfer rate of CO_2 (F) is given by

$$F = I \times (pCO_{2sea} - pCO_{2air})/pCO_{2air} = F_{12} \times \Delta pCO_2/pCO_{2air} \quad \text{(B5)}$$

In this case, the sign of F (or direction of flux) is *positive upwards*. Thus the net flux of CO_2 will be from sea to air, in regions where ΔpCO_2 is positive. This condition is common in most tropical oceanic areas due to equatorial upwelling, which brings deeper CO_2 rich waters to the surface. The exchange rates calculated from bomb-^{14}C inventories are the long-term averaged values. Thus, if average ocean-atmosphere pCO_2 gradient (ΔpCO_2) over a given oceanic region is known, it is possible to compute the net transfer rate of CO_2 from the exchange rates. Based on the uncertainties in the ^{14}C-based exchange rates (20%) and in the estimates of ΔpCO_2 (10%) the maximum uncertainty on F is expected to be within 30%.

[32] **Acknowledgments.** We are very much indebted to B. L. K. Somayajulu for his support and guidance, who was inspiration in initiation of this program. Critical comments and suggestions from S. Krishnaswami and two anonymous reviewers greatly helped in improving this paper. We are thankful to the Captain and crew of FORV *Sagar Sampada* for providing all onboard logistics support and large volume sampling. We are thankful to the Ministry of Earth Sciences (previously Department of Ocean Development), Government of India, for providing ship time. We are grateful to the Director and staff of Centre of Marine Living Resources, Cochin for helping in managing the various cruises and the technical staff of NORINCO for providing help in onboard instrument operation. The onboard help provided by J. P. Bhavsar and R. Agnihotri is sincerely acknowledged. Authors are grateful to M. Dileep Kumar for his critical suggestions.

References

Bard, E., M. Arnold, G. H. Ostlund, P. Maurice, P. Monfray, and J.-C. Duplessy (1988), Penetration of bomb radiocarbon in the tropical Indian Ocean measured by means of accelerator mass spectrometry, *Earth Planet. Sci. Lett.*, *87*, 379–389, doi:10.1016/0012-821X(88)90002-7.

Bard, E., M. Arnold, J. R. Toggweiler, P. Maurice, and J.-C. Duplessy (1989), Bomb ^{14}C in the Indian Ocean measured by accelerator mass spectrometry: Oceanographic implications, *Radiocarbon*, *31*, 510–522.

Bates, N. R., A. C. Pequignet, and C. L. Sabine (2006), Ocean carbon cycling in the Indian Ocean: 1. Spatiotemporal variability of inorganic carbon and air-sea CO_2 gas exchange, *Global Biogeochem. Cycles*, *20*, GB3020, doi:10.1029/2005GB002491.

Bhushan, R., S. Chakraborty, and S. Krishnaswami (1994), Physical Research Laboratory (Chemistry) Radiocarbon date list, *Radiocarbon*, *36*(2), 251–256.

Bhushan, R., S. Krishnaswami, and B. L. K. Somayajulu (1997), ^{14}C in air over the Arabian Sea, *Curr. Sci.*, *73*, 273–276.

Bhushan, R., B. L. K. Somayajulu, S. Chakraborty, and S. Krishnaswami (2000), Radiocarbon in the Arabian Sea water column: Temporal variations in bomb ^{14}C inventory since the GEOSECS and CO_2 air-sea exchange rates, *J. Geophys. Res.*, *105*, 14,273–14,282, doi:10.1029/2000JC000255.

Bhushan, R., K. Dutta, S. Mulsow, P. P. Povinec, and B. L. K. Somayajulu (2003), Distribution of natural and man-made radionuclides during reoccupation of GEOSECS stations 413 and 416 in the Arabian Sea: Temporal changes, *Deep Sea Res., Part II*, *50*, 2777–2784, doi:10.1016/S0967-0645(03)00147-4.

Broecker, W. S., T.-H. Peng, H. G. Östlund, and M. Stuiver (1985), The distribution of bomb radiocarbon in the ocean, *J. Geophys. Res.*, *90*, 6953–6970, doi:10.1029/JC090iC04p06953.

Broecker, W. S., S. Sutherland, W. Smethie, T.-H. Peng, and H. G. Östlund (1995), Oceanic radiocarbon: Separation of the natural and bomb components, *Global Biogeochem. Cycles*, *9*, 263–288, doi:10.1029/95GB00208.

Cember, R. (1989), Bomb radiocarbon in the Red Sea: A medium-scale gas exchange experiment, *J. Geophys. Res.*, *94*, 2111–2123, doi:10.1029/JC094iC02p02111.

Chakraborty, S., R. Ramesh, and S. Krishnaswami (1994), Air-sea exchange of CO_2 in the Gulf of Kutch, northern Arabian Sea based on bomb-carbon in corals and tree rings, *Proc. Indian Acad. Sci., Earth Planet. Sci.*, *103*, 231–242.

Chakraborty, S., K. Dutta, A. Bhattacharyya, M. Nigam, E. A. G. Schuur, and S. K. Shah (2008), Atmospheric ^{14}C variability recorded in tree rings from peninsular India: Implications for fossil fuel CO_2 emission and atmospheric transport, *Radiocarbon*, *50*(3), 321–330.

da Silva, A. M., C. C. Young-Molling, and S. Levitus (1994), *Atlas of Surface Marine Data 1994*, vol. 1, *Algorithms and Procedures*, *NOAA Atlas NESDIS*, vol. 6, 83 pp., NOAA, Silver Spring, Md.

Druffel, E. R. M. (1989), Decade time scale variability of ventilation in the North Atlantic: High-precision measurements of bomb radiocarbon in banded corals, *J. Geophys. Res.*, *94*, 3271–3285, doi:10.1029/JC094iC03p03271.

Druffel, E. R. M., and S. Griffin (2008), Daily variability of dissolved inorganic radiocarbon at three sites in the surface ocean, *Mar. Chem.*, *110*, 185–189, doi:10.1016/j.marchem.2008.04.004.

Dutta, K. (2001), Study of marine processes in the Northern Indian Ocean using radiocarbon, PhD thesis, MS, pp. 168, Univ. of Baroda, Vadodara, India.

Dutta, K., R. Bhushan, and B. L. K. Somayajulu (2001), Δ-R correction values for the northern Indian Ocean, *Radiocarbon*, *43*(2a), 483–488.

Dutta, K., R. Bhushan, B. L. K. Somayajulu, and N. Rastogi (2006), Interannual variation in atmospheric $\Delta^{14}C$ over the Northern Indian Ocean, *Atmos. Environ.*, *40*, 4501–4512, doi:10.1016/j.atmosenv.2006.04.013.

Dutta, K., R. Bhushan, and B. L. K. Somayajulu (2007), Rapid vertical mixing rates in deep waters of the Andaman Basin, *Sci. Total Environ.*, *384*, 401–408, doi:10.1016/j.scitotenv.2007.04.041.

Dutta, K., G. V. Ravi Prasad, D. K. Ray, and S. Raghav (2010), Decadal changes of radiocarbon in the surface Bay of Bengal: Three decades after GEOSECS and one decade after WOCE, *Radiocarbon*, *52*(3), 1191–1196.

Feely, R., R. Wanninkhof, W. McGillis, M.-E. Carr, and C. E. Cosca (2004), Effects of wind speed and gas exchange parameterizations on the air-sea CO_2 fluxes in the equatorial Pacific Ocean, *J. Geophys. Res.*, *109*, C08S03, doi:10.1029/2003JC001896.

Fine, R. A. (1985), Direct evidence using tritium data for throughflow from the Pacific into the Indian Ocean, *Nature*, *315*, 478–480, doi:10.1038/315478a0.

Goyet, C., C. Coatanoan, G. Eischeid, T. Amaoka, K. Okuda, R. Healy, and S. Tsunogai (1999), Spatial variation of total CO_2 and total alkalinity in the northern Indian Ocean: A novel approach for the quantification of anthropogenic CO_2 in seawater, *J. Mar. Res.*, *57*, 135–163, doi:10.1357/002224099765038599.

Gruber, N., et al. (2009), Oceanic sources, sinks, and transport of atmospheric CO_2, *Global Biogeochem. Cycles*, *23*, GB1005, doi:10.1029/2008GB003349.

Guilderson, T. P., K. Caldeira, and P. B. Duffy (2000), Radiocarbon as diagnostic tracer in ocean and carbon cycle modeling, *Global Biogeochem. Cycles*, *14*, 887–902, doi:10.1029/1999GB001192.

Gupta, S. K., and H. A. Polach (1985), *Radiocarbon Dating Practices at ANU, Radiocarbon Lab. Handb.*, *Res. Sch. Pac. Stud.*, 173 pp., Aust. Natl. Univ., Canberra, Australia.

Hua, Q., and M. Barbetti (2004), Review of tropospheric bomb ^{14}C data for carbon cycle modeling and age calibration purposes, *Radiocarbon*, *46*(3), 1273–1298.

Jain, A. K., H. S. Kheshgi, M. I. Hoffert, and D. J. Wuebbles (1995), Distribution of radiocarbon as a test of global carbon cycle models, *Global Biogeochem. Cycles*, *9*, 153–166, doi:10.1029/94GB02394.

Karlen, I., I. U. Olsson, P. Kallburg, and S. Kilici (1968), Absolute determination of the activity of two ^{14}C dating standards, *Ark. Geofys.*, *4*, 465–471.

Körtzinger, A., J. C. Duinker, and L. Mintrop (1997), Strong CO_2 emissions from the Arabian Sea during South-West Monsoon, *Geophys. Res. Lett.*, *24*(14), 1763–1766, doi:10.1029/97GL01775.

Körtzinger, A., K. M. Johnson, L. Mintrop, J. C. Duinker, and D. W. R. Wallace (1999), Coulometric total carbon dioxide analysis for marine studies: Measurement and internal consistency of underway TCO_2 concentrations, *Mar. Chem.*, *67*(1–2), 123–144.

Kumar, M. D., A. Rajendran, K. Somasundar, V. Ittekot, and B. N. Desai (1992), Processes controlling carbon components in the Arabian Sea, in

Oceanography of the Indian Ocean, edited by B. N. Desai, pp. 313–325, Oxford, New Delhi.

Kumar, M. D., S. W. A. Naqvi, M. D. George, and D. A. Jayakumar (1996), A sink for atmospheric carbon dioxide in the northeast Indian Ocean, *J. Geophys. Res.*, *101*, 18,121–18,125, doi:10.1029/96JC01452.

Louanchi, F., N. Metzl, and A. Poisson (1996), Modelling the monthly sea surface f_{CO2} fields in the Indian Ocean, *Mar. Chem.*, *55*, 265–279, doi:10.1016/S0304-4203(96)00066-7.

Noakes, J. E., S. Kim, and J. J. Stipp (1965), Chemical and counting advances in liquid scintillation age dating, in *Proceedings of 6th International Conference on ^{14}C and Tritium Dating*, *USAEC 650-652*, edited by R. M. Chatter and E. A. Olson, pp. 68–92, Natl. Bur. Stand., Washington, D. C.

Nydal, R., and K. Lövseth (1996), Carbon-14 measurements in atmospheric CO_2 from Northern and Southern Hemisphere sites, 1962–1993, *NDP-057*, Carbon Dioxide Inf. Anal. Cent., Oak Ridge Natl. Lab., Oak Ridge, Tenn.

Peacock, S. (2004), Debate over the ocean bomb radiocarbon sink: Closing the gap, *Global Biogeochem. Cycles*, *18*, GB2022, doi:10.1029/2003GB002211.

Peng, T.-H., R. M. Key, and H. G. Östlund (1998), Temporal variations of bomb radiocarbon inventory in the Pacific Ocean, *Mar. Chem.*, *60*, 3–13, doi:10.1016/S0304-4203(97)00089-3.

Povinec, P. P., S. H. Lee, L. L. W. Kwong, B. Oregioni, A. J. T. Jull, W. E. Kieser, U. Morgenstern, and Z. Top (2010), Tritium, radiocarbon, ^{90}Sr and ^{129}I in the Pacific and Indian Oceans, *Nucl. Instrum. Methods Phys. Res., Sect. B*, *268*(7–8), 1214–1218, doi:10.1016/j.nimb.2009.10.136.

Quay, P. D., and M. Stuiver (1980), Vertical advection–diffusion rates in the oceanic thermocline determined from ^{14}C distributions, *Radiocarbon*, *22*, 607–625.

Rafter, T. A., and G. J. Ferguson (1957), "Atomic bomb effect"—Recent increase of carbon-14 content of the atmosphere and biosphere, *Science*, *126*, 557–558, doi:10.1126/science.126.3273.557.

Ravi Prasad, G. V., K. Dutta, and D. K. Ray (2008), Radiocarbon AMS at IOP: System improvements and dating of groundwater from Bhadrak district, Orissa, *Nucl. Instrum. Methods Phys. Res., Sect. B*, *266*(8), 1833–1836, doi:10.1016/j.nimb.2007.11.060.

Rubin, S. I., and R. Key (2002), Separating natural and bomb-produced radiocarbon in the ocean: The potential alkalinity method, *Global Biogeochem. Cycles*, *16*(4), 1105, doi:10.1029/2001GB001432.

Sarma, V. V. S. S., M. D. Kumar, and M. D. George (1998), The central and the eastern Arabian Sea as a perennial source of atmospheric carbon dioxide, *Tellus, Ser. B*, *50*, 179–184, doi:10.1034/j.1600-0889.1998.t01-1-00005.x.

Sarma, V. V. S. S., M. D. Kumar, M. Gauns, and M. Madhupratap (2000), Seasonal controls on surface pCO_2 in the central and eastern Arabian Sea, *Proc. Indian Acad. Sci., Earth Planet. Sci.*, *109*, 471–479.

Somayajulu, B. L. K., R. Bhushan, and P. V. Narvekar (1999), $\Delta^{14}C$, ΣCO_2 and salinity of the western Indian Ocean deep waters: Spatial and temporal variations, *Geophys. Res. Lett.*, *26*(18), 2869–2872, doi:10.1029/1999GL002261.

Southon, J., M. Kashgarian, M. Fontugne, B. Metivier, and W. W.-S. Yim (2002), Marine reservoir corrections for the Indian Ocean and southeast Asia, *Radiocarbon*, *44*(1), 167–180.

Strickland, J. D. H., and T. R. Parsons (1972), *A Practical Handbook of Sea-Water Analysis*, Fish. Res. Board of Can., Ottawa.

Stuiver, M. (1980), ^{14}C distribution in Atlantic Ocean, *J. Geophys. Res.*, *85*, 2711–2718, doi:10.1029/JC085iC05p02711.

Stuiver, M., and H. A. Polach (1977), Discussion: Reporting of ^{14}C data, *Radiocarbon*, *19*(3), 355–363.

Stuiver, M., and H. G. Östlund (1983), GEOSECS Indian Ocean and Mediterranean radiocarbon, *Radiocarbon*, *25*, 1–29.

Stuiver, M., P. D. Quay, and T. F. Braziunas (2000), Isotope and carbon cycle inferences, in *The Carbon Cycle*, edited by T. M. L. Wigley and D. S. Schimel, pp. 153–160, Cambridge Univ. Press, Cambridge, U. K., doi:10.1017/CBO9780511573095.014.

Sweeney, C., E. Gloor, A. R. Jacobson, R. M. Key, G. McKinley, J. L. Sarmiento, and R. Wanninkhof (2007), Constraining global air-sea gas exchange for CO_2 with recent bomb ^{14}C measurements, *Global Biogeochem. Cycles*, *21*, GB2015, doi:10.1029/2006GB002784.

Takahashi, T., et al. (2009), Climatological mean and decadal changes in surface ocean pCO_2, and net sea-air CO_2 flux over the global oceans, *Deep Sea Res., Part II*, *56*, 554–577, doi:10.1016/j.dsr2.2008.12.009.

Toggweiler, J. R., and S. Trumbore (1985), Bomb-test ^{90}Sr in Pacific and the Indian Ocean surface water as recorded by banded corals, *Earth Planet. Sci. Lett.*, *74*, 306–314, doi:10.1016/S0012-821X(85)80002-9.

Toggweiler, J. R., K. Dixon, and K. Bryan (1989), Simulations of radiocarbon in a coarse-resolution world ocean model, 2. Distributions of bomb-produced Carbon-14, *J. Geophys. Res.*, *94*, 8243–8264, doi:10.1029/JC094iC06p08243.

Wanninkhof, R. (1992), Relationship between wind speed and gas exchange over the ocean, *J. Geophys. Res.*, *97*, 7373–7382, doi:10.1029/92JC00188.

Wanninkhof, R., and W. R. McGillis (1999), A cubic relationship between air-sea CO_2 exchange and wind speed, *Geophys. Res. Lett.*, *26*, 1889–1892, doi:10.1029/1999GL900363.

Wanninkhof, R., J. Ledwell, and W. S. Broecker (1985), Gas exchange-wind speed relation measured with sulfur hexafluoride on a lake, *Science*, *227*, 1224–1226, doi:10.1126/science.227.4691.1224.

Weiss, R. F. (1974), Carbon dioxide in water and seawater: The solubility of a non-ideal gas, *Mar. Chem.*, *2*, 203–215.